5874 *Biochemistry* **2009,** *48,* 5874–5881
DOI: 10.1021/bi802280b

BIOCHEMISTRY
including biophysical chemistry & molecular biology
Article

Interfacial Mechanism of Phospholipase A_2: pH-Dependent Inhibition and Me-β-cyclodextrin Activation

Hanna P. Wacklin*

Australian Nuclear Science and Technology Organisation, PMB1, Menai, NSW 2234, Australia and Institut Laue Langevin, BP 156, 38042 Grenoble Cedex 9, France

Received December 15, 2008; Revised Manuscript Received May 6, 2009

ABSTRACT: The pH-dependent activity of phospholipase A_2 (PLA_2) from *Naja mossambica mossambica* venom and the membrane-water partitioning of the lipid hydrolysis products were investigated in solid-supported palmitoyl-oleyl-phosphatidylcholine-d_{31} (POPC-d_{31}) membranes using neutron reflection. At pH 5, PLA_2 interacts only weakly with the substrate membrane and leads to no observable membrane breakdown, which is consistent with protonation of the catalytic histidine (His48, $pK_a \sim 6.2$). The rate of the lyso-lipid partitioning into the solution phase is the same at pH 9 as at pH 7.4, and the relative membrane-water partitioning of the products is essentially the same; that is, the fatty acid accumulates in the membrane, and only the lyso-lipid is solubilized. However, Me-β-cyclodextrin (Me-β-CD) activates PLA_2 irrespective of pH by facilitating the solubilization of the lyso-lipid product, but not the fatty acid, of which only 22% is encapsulated at pH 9. Since no product solubilization is observed at pH 5 in the absence of Me-β-CD, this suggests that the hydrolytic mechanism of PLA_2 is not fully disabled at pH 5 but is inhibited by a mechanism, which is counteracted by Me-β-CD-mediated release of the lyso-lipid. Me-β-CD does not interact with the substrate membrane, which indicates that at low pH the product extraction occurs directly from the enzyme active site outside the immediate membrane−water interface, whereas at pH 7−9, direct solubilization of the lyso-lipid from the membrane can also contribute to activation of PLA_2.

Phospholipase A_2 (PLA_2)[1] enzymes (*1*) selectively cleave the *sn*-2 acyl chain in L-α-1,2-diacyl-*sn*-glycerophospholipids, releasing a fatty acid and a lyso-phospholipid, both of which are precursors to important biochemical signaling agents such as the eicosanoids (*2*, *3*). PLA_2 enzymes hydrolyze naturally occurring phospholipids as well as synthetic analogues with a variety of chemical structures, but only do so when the substrate molecules are in aggregated form, that is, in a bilayer membrane, monolayer, or micelles. The heterogeneous nature of PLA_2 catalysis and its wide range of physiological functions have given the mechanism the status of a paradigm in interfacial enzymology (*4*).

The interfacial nature of PLA_2 hydrolysis means that conventional kinetic schemes cannot readily be used to analyze the reaction. Although the membrane and enzyme form a heterogeneous system otherwise analogous to surface catalysis, the enzyme partitioning between the membrane and the aqueous phase may change as the insoluble lipid reaction products, a fatty acid and a lyso-phosphocholine, accumulate in the membrane.

It has been shown previously that the integrity of the substrate membrane is compromised once a significant fraction of the lipids have reacted, which demonstrates that the reaction products alter the membrane morphology, and also suggests that some or all of the products may partition out of the membrane, but methods to directly measure this have been limited. PLA_2 digestion of supported membranes leads to the formation of holes and defects (*5*, *6*), which subsequently grow larger. Phospholipid vesicles initially shrink (*7*) before being degraded into micelles (*8*) or disks (*9*), which may also be accompanied by fusion into micrometer-large aggregates. Monolayers of short chain phospholipids are hydrolyzed in a manner that suggests not all the reaction products are immediately solubilized (*10*, *11*). Cyclodextrins activate PLA_2 (*12*), and it has been suggested that this is based on removal of the reaction products as inclusion complexes, as the products have been shown to have both autocatalytic and autoinhibitory effects on the enzyme.

Many detailed investigations have been dedicated to elucidating the effects of the products on PLA_2 activity, when they are added to the substrate membrane a priori. An activating effect of the products was discovered by Jain and co-workers during extensive studies of porcine pancreatic PLA_2 (*13*), and was suggested to be related to a change in the bilayer phase transition temperature T_m, and/or stabilization of defects that enhance PLA_2 binding. PLA_2 activation is more sensitive to the nature of the fatty acid than the lyso-lipid, which only has an activating effect if added to the aqueous phase (*14*), rather than premixed into the substrate vesicles (*15*, *16*).

It was identified by Apitz-Castro et al. (*15*) that a critical mole fraction of reaction products is required to abolish the inactive lag phase of pancreatic PLA_2, and it was determined later that the

*To whom correspondence should be addressed. E-mail: wacklin@ill.eu. Tel.: +33 (0) 476 20 7738. Fax: +33 (0) 476 20 7120.

[1]Abbreviations: POPC-d_{31} = L-α-1-*O*-d_{31}-palmitoyl,2-*O*-oleyl,3-*O*-*sn*-glycerophosphocholine, PLA_2 = phospholipase A_2, Me-β-CD = methyl-β-cyclodextrin.

 Published on Web 05/06/2009

critical fraction corresponds to the region where the products start to cause lateral segregation in the membrane(*17*). It has also been shown that the inactive lag phase of pancreatic PLA_2 is shortest at the membrane phase transition temperature (*18*, *19*), when defects form spontaneously (*20*, *21*).

Detailed studies into how the individual reaction products alter PLA_2 binding and the catalytic rate (*22*−*24*) have revealed a complex relationship between the products. In particular, addition of both products together decreases the critical product fraction required for activation, compared to addition of either product on its own. Fatty acid primarily promotes PLA_2 binding, but lyso-lipid also has a partially inhibiting effect.

Although most of the work on product activation of PLA_2 has been concerned with pancreatic PLA_2, the membrane properties that are believed to be the causative effect, such as the membrane fluidity and homogeneity, are properties of the membrane lipids, and thus play a role in the activity of all PLA_2 enzymes. Progress in understanding the interfacial mechanism and activation of PLA_2 enzymes has been limited by the substrates (vesicles or micelles) and techniques (pH titration, fluorescence assays) used, with which it is not possible to probe membrane structure or determine the effects of the products as they are generated in the membrane.

A new method to measure the membrane concentrations of the lipids, PLA_2, and the reaction products as they are generated in situ by neutron reflection was developed recently (*25*). The method uses a selectively sn1-chain deuterated lipid, palmitoyl-oleyl-phosphatidylcholine-d_{31} (POPC-d_{31}), which is cleaved by PLA_2 into oleic acid and deuterated lyso-d_{31}-palmitoyl-phosphocholine (lyso-PC). As the fragments have neutron scattering length densities that are distinguishable from the substrate lipid, neutron reflection allows their amounts in the membrane to be determined directly during the reaction, as well as measuring the structure of the membrane and the number of enzyme molecules bound to it. The sensitivity of neutron reflectivity to the relative amount of the fatty acid and deuterated lyso-lipid in the membrane during PLA_2 hydrolysis is demonstrated in the Supporting Information. Previously, a non-deuterated POPC substrate was used to determine that approximately 50% of the substrate mass is destroyed by PLA_2 from *Naja mossambica mossambica* venom (*26*), whereas using POPC-d_{31} showed that all the deuterated lyso-PC partitions into the aqueous phase, while the remaining membrane is composed of oleic acid and PLA_2 (*25*).

In this paper, the relationship between the pH-dependent activity of PLA_2 and the membrane−water partitioning of the reaction products is investigated. The motivation for studying the pH dependence arose from the fact that there may be changes in the solubility of the fatty acid product (pK_a 7−8), which becomes more negatively charged with increasing pH. As a control, Me-β-cyclodextrin (Me-β-CD) was used to extract the reaction products under identical conditions to determine other pH-dependent changes in the enzyme−membrane interaction.

MATERIALS AND METHODS

Neutron Reflection. Details of the analysis of supported lipid membrane structure (*27*) and lipid hydrolysis by PLA_2 (*26*) using time-of-flight neutron reflection have been described previously. Briefly, the neutron scattering length density profile $\rho(z)$ of a lipid bilayer can be divided into separate headgroup and acyl chain regions due to their chemical differences and water penetration.

Table 1: Molecular Volumes V and Neutron Scattering Length Densities ρ Used in Fitting Data and Calculating Bilayer Compositions

compound	V/ Å^3	ρ/ 10^{-6} Å^{-2}
POPC-d_{31}	1256[a]	0.27[c]
headgroups	322[a]	1.8[c]
chains	933[a]	3.2[c]
PLA_2	15451[b]	3.6[b]
oleic acid	467[d]	−0.3[c]
lyso-C16:0-PC	789[d]	6.8[c]
D_2O	30	6.35
CmSi	30	2.07

[a] From molecular dynamic simulations, as detailed previously (*26*). [b] Calculated from the sequence of *Naja mossambica mossambica* PLA_2 using values for aqueous protein solutions, taking into account the number of exchangeable protons. [c] Calculated from the molecular volumes and coherent nuclear scattering lengths of the molecules. [d] The volume of oleic acid is estimated to be half of the total chain volume of POPC-d_{31} and that of the lyso-PC the volume of POPC-d_{31}−oleic acid.

Reflectivity analysis is based on modeling the thickness, scattering length density, lipid volume fraction, and roughness of four layers corresponding to the lipid head groups, the acyl chain region, and PLA_2, which resides at the membrane−water interface with partial penetration into the outer membrane leaflet (*26*). A simple molecular volume-based constraint, which assumes that the total surface area covered by the membrane is the same on both sides of the bilayer, ensures the correct distribution of the water molecules associated with the membrane and maintains the area per molecule constant across the bilayer. In membranes containing phosphoplipid (PL), fatty acid (FA), and lysolipid (LPC), the scattering length density ρ_{layer} is the sum of the molecular scattering length densities ρ_i weighted by the volume fractions φ_i of each component and water (W):

$$\rho_{layer} = \phi_{PL}\rho_{PL} + \phi_{LPC}\rho_{LPC} + \phi_{FA}\rho_{FA} + \phi_{W}\rho_{W} \quad (1)$$

Thus, when there are significant differences in the molecular scattering length densities of PL, LPC, FA, and water, their individual volume fractions can be computed from the fitted scattering length density of the layer. In the present work, a D_2O subphase was used, as it gives the highest contrast to the partially deuterated lipids, the enzyme, and the silicon support. It was still possible to distinguish between the deuterated lyso-lipid product and the D_2O solvent because of the nondeuterated glycerophosphocholine headgroups.

The Motofit program (*28*) was used for optical matrix modeling (*29*) to calculate specular reflectivity from model structures. The scattering length densities of phospholipid, lyso-lipid, fatty acid, and PLA_2 were calculated as described previously (*25*) and are listed in Table 1. The errors in the structural parameters of each sublayer were derived from the maximum acceptable variation in the fitted thickness and lipid volume fraction that allowed a fit to be maintained, subject to the constant molecular area constraint. However, the errors in independent parameters of the model sublayers are coupled in such a way that the overall errors in membrane volume fraction and thickness are ±10% and ±2 Å, respectively.

Experimental Procedures. Specular neutron reflection was measured on the SURF reflectometer at the ISIS Neutron and Muon Facility, Rutherford Appleton Laboratory, UK, and the D17 reflectometer at the Institut Laue Langevin (ILL), Grenoble, France, using neutron wavelengths λ of 0.5−6 Å (at ISIS) and 2−19 Å (at ILL) to record reflectivity profiles between

$0.01 < Q < 0.5$ Å^{-1}, where $Q = (4\pi \sin\theta)/\lambda$ is the momentum transfer vector of the neutrons in the direction (z) perpendicular to the membrane-water interface. Under these conditions, a typical measurement at two to three incident angles (0.35°, 0.8°, and 1.8° at ISIS and 0.8° and 3° at ILL) to obtain the full reflectivity profile required 60−70 min. The phospholipid bilayers were formed in the neutron reflectometer sample chamber after measuring the structure of the underlying Si-SiO_2 surface in two contrasts (D_2O and water contrast matched to silicon CmSi, sld = 2.07×10^{-6} Å^{-2}). Each lipid membrane structure was also measured in D_2O and CmSi contrasts before exposure to PLA_2.

Materials. POPC-d_{31} was purchased from Avanti Polar Lipids. Phospholipase A_2 from *Naja mossambica mossambica* venom (P7778, ~90% purity, 1500 units per mg), Me-β-CD, Tris-HCl, and D_2O (>99%) were purchased from Sigma-Aldrich. Ultrahigh quality water (R = 18.2 MΩ·cm) was used in all experiments and surface preparations. The support surfaces (silicon [111] orientation) were polished in house and cleaned by a 1:4:5 solution of $H_2O_2/H_2SO_4/H_2O$ at 80 °C followed by UV ozonolysis prior to the experiment. This treatment generates a highly hydrophilic native SiO_2 layer of 7−15 Å thickness and 3−5 Å roughness.

Supported Membrane Formation. Phospholipid bilayers were formed by adsorption of sonicated small unilamellar vesicles of POPC-d_{31} (0.5 mg/mL) to a silicon surface preheated to 35 °C with an incubation period of 1−2 h prior to rinsing off the excess vesicles and cooling to 25 °C. All PLA_2 and Me-β-CD experiments were carried out at 25 °C, at a PLA_2 concentration of 0.01 mg/mL, in the absence and presence of 0.5 mg/mL Me-β-CD (which was premixed into the PLA_2 solution). This concentration of Me-β-CD was chosen on the basis of previously published studies, which have shown that similar concentrations lead to desorption of fatty acids from monolayers (*30*) and activate PLA_2 (*31*) as well as other lipases (*12*).

RESULTS

POPC-d_{31} Hydrolysis As a Function of pH. The reflectivity profiles recorded during the hydrolysis of POPC-d_{31} at pH 5 and pH 9 by 0.01 mg/mL PLA_2 are shown in Figure 1, with the scattering length density profiles corresponding to the best fits shown in the insets. The fitted lipid scattering length densities, thicknesses, and volume fractions (ρ, t, ϕ) and the structural parameters derived from them (area per molecule, A, and surface coverage, Γ) corresponding to the fits, are listed in Table 2. There is no difference in the structure or quality of the substrate membranes between the two experiments; both have a high surface coverage (98%) and an area per molecule of 61 ± 6 Å^2, which is typical for POPC in the liquid crystalline phase. The membrane coverage of 98% corresponds to the lipid volume fraction (ϕ = 0.98 ± 0.02) in the hydrocarbon chain region and reflects the specific volume assigned to the lipid chains. In this case, a specific chain volume derived from molecular dynamics simulations of POPC at 25 °C was used, and it is possible that the value for lipids in a supported membrane differs by a small amount due to the lipid−surface interactions. The statistical uncertainty in the data also leads to a fitting error of ~2% in the lipid volume fraction and a propagated error of ±6 Å or 10% in the area per lipid molecule. Thus, it is not possible to assign the 2% of membrane volume to physical defects.

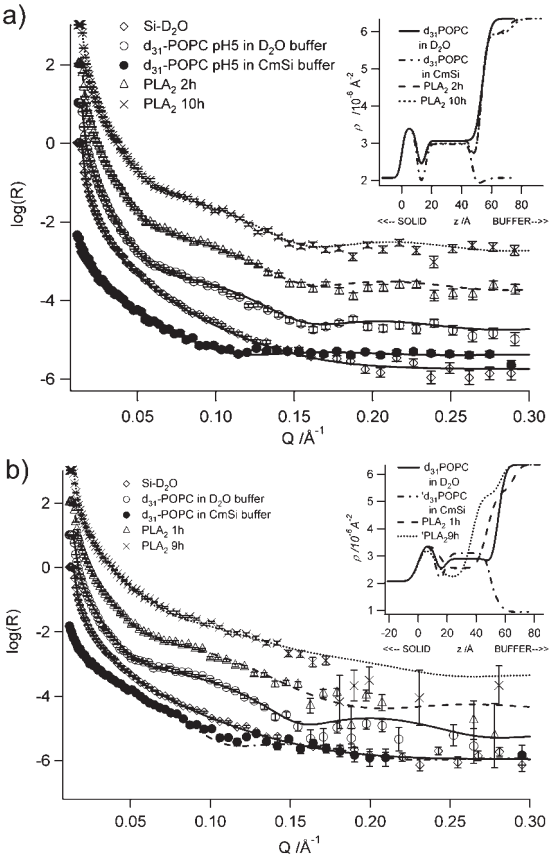

FIGURE 1: Neutron reflectivity profiles recorded before and during POPC-d_{31} hydrolysis by 0.01 mg/mL PLA_2 at (a) pH 5 and (b) pH 9. The fitted reflectivity curves (lines) and scattering length density profiles (in inset) correspond to the model parameters listed in Table 2.

At pH 5, changes in reflectivity after PLA_2 injection are very small and correspond to 0.03 ± 0.01 μmol m^{-2} of PLA_2, which adsorbed to the membrane−water interface within the first 2 h but did not cause any observable decrease in the membrane lipid volume fraction or composition within 10 h. Although it is not possible to say directly from the data that no hydrolysis occurred, it is unlikely that a significant fraction of products were formed, as the solubility of the lyso-lipid is unchanged at pH 5, and it would partition into the solution phase (the fitting resolution for ρ_{chains} in this contrast ± 0.1×10^{-6} Å^{-2}, which corresponds to a detection limit of 0.03 for the mole fraction of lyso-lipid solubilized).

At pH 9, the lipid volume fraction started to decrease within 1 h, with considerably more (0.08 ± 0.01 μmol m^{-2}) PLA_2 initially adsorbed on the membrane surface. After 9 h, the membrane had been completely digested into a fatty acid layer of 21 ± 3 Å (sld = $-0.3 \pm 0.1 \times 10^{-6}$ Å^{-2}), with 0.14 ± 0.03 μmol m^{-2} PLA_2 attached to the lipid−water interface. Comparison of this result with previous data measured at pH 7.4 (*25*) reveals that the reaction rate is not significantly different at pH 9 than at neutral pH.

At pH 9, the scattering length density ρ_{chains} of the lipid decreased from $3.0 \pm 0.1 \times 10^{-6}$ Å^{-2} to $1.6 \pm 0.1 \times 10^{-6}$ Å^{-2} within 1 h, which corresponds to the hydrolysis 42% of the phospholipids and partitioning of all the lyso-lipid into the solution phase. At pH 7.4, ρ_{chains} decreased from $3.17 \pm 0.1 \times 10^{-6}$ Å^{-2} to $1.44 \pm 0.1 \times 10^{-6}$ Å^{-2} within 70 min, which agrees with the pH 9 results to within the errors in determining ρ_{chains}. There was no

Table 2: Structural Parameters of POPC-d_{31} Bilayers before and after PLA_2 Hydrolysis at pH 5 and pH 9

description	layer	ρ/ 10^{-6} Å^{-2}[a]	ρ_a/ 10^{-6} Å^{-2}[b]	t/ Å[c]	ϕ[d]	A_a/ Å[e]	Γ/ μmol m^{-2}[f]
POPC-d_{31} pH 5	head 1	1.8	2.3 ± 0.2	6 ± 1	0.88 ± 0.05	61 ± 16	
	chains	3.0 ± 0.15	3.1 ± 0.1	31 ± 2	0.98 ± 0.02	61 ± 6	5.4 ± 0.5
	head 2	1.8	2.9 ± 0.2	7 ± 1	0.75 ± 0.05	61 ± 15	
POPC-d_{31} pH 5 + PLA_2 10 h	head 1	1.8	2.3 ± 0.2	6 ± 1	0.88 ± 0.05	61 ± 16	
	chains	3.0 ± 0.15	3.1 ± 0.1	31 ± 2	0.98 ± 0.02	61 ± 6	5.4 ± 0.5
	head 2	1.8	2.9 ± 0.2	7 ± 1	0.75 ± 0.05	61 ± 15	
	PLA_2	3.6	5.9 ± 0.1	21 ± 3	0.15 ± 0.07	5700 ± 3300	0.03 ± 0.01
POPC-d_{31} pH 9	head 1	1.8	2.3 ± 0.2	6 ± 1	0.88 ± 0.05	61 ± 16	
	chains	3.0 ± 0.15	3.1 ± 0.1	31 ± 2	0.98 ± 0.02	61 ± 6	5.4 ± 0.5
	head 2	1.8	2.9 ± 0.2	7 ± 1	0.88 ± 0.05	61 ± 14	
POPC-d_{31} pH 9 + PLA_2 1 h	head 1	1.8	3.1 ± 0.2	7 ± 1	0.75 ± 0.05	88 ± 29	
	chains	1.6 ± 0.15	2.6 ± 0.1	27 ± 2	0.79 ± 0.02	88 ± 9	3.8 ± 0.4
	head 2	2.2	3.3 ± 0.2	5 ± 1	0.73 ± 0.05	88 ± 29	
	PLA_2	3.6	5.4 ± 0.2	22 ± 3	0.35 ± 0.07	2000 ± 700	0.08 ± 0.02
POPC-d_{31} pH 9 + PLA_2 9 h	FA[g]	−0.3 ± 0.15	2.2 ± 0.2	25 ± 1	0.62 ± 0.02	30 ± 4	5.5 ± 0.6
	PLA_2	3.6	2.8 ± 0.2	21 ± 3	0.60 ± 0.07	1200 ± 350	0.14 ± 0.03

[a] ρ = molecular scattering length density. Where no error limits for ρ are given, the parameters were fixed in our data-analysis. [b] ρ_a = total scattering length density of layer a, including D_2O. Head 1 refers to the inner headgroup layer facing the silicon surface. [c] t = layer thickness. [d] ϕ = lipid volume fraction. [e] A_a is the area available per molecule. [f] Γ is the lipid surface coverage. [g] FA = fatty acid. This layer is assumed to be composed only of oleic acid, and the values of A_a and Γ have been calculated using the molecular volume of 467 Å^3 corresponding to it.

difference in the solubilization of the oleic acid/oleate between pH 7.4 and pH 9, despite its increasing ionization, and it all remained bound to the silicon support surface. This is evident from the surface coverage of the oleic acid/oleate layer, which corresponds to the same number of molecules as in the original lipid bilayer. These fatty acid bilayers are consistent with the pH region 7−9 being favorable for the formation the acid−soap complexes between the ionized and un-ionized forms of the acid, which has the effect of stabilizing the bilayer geometry, as well as increasing the apparent pK_a of long chain fatty acids(*32*, *33*).

POPC-d_{31} Hydrolysis in the Presence of Me-β-CD. To determine the effects of changing pH on PLA_2 activity and the enzyme−membrane interaction independently of the solubility of the reaction products, hydrolysis of POPC-d_{31} was also investigated in the presence of Me-β-CD, which has been shown to extract fatty acids from monolayers at the air−water interface (*30*, *34*) and to have an activating effect on PLA_2 and other lipase enzymes(*12*, *31*).

Figure 2 shows the neutron reflectivity and scattering length density profiles measured during POPC-d_{31} hydrolysis in the presence of 0.5 mM Me-β-CD. In contrast to the results obtained without Me-β-CD, the hydrolysis is complete within 1 h at all three pH values. The results in Table 3 show that in each case, a nearly identical fatty acid layer remains on the silicon surface, but the amount of PLA_2 bound to it increased with pH from 0.08 ± 0.03 μmol m^{-2} at pH 5 to 0.12 ± 0.03 μmol m^{-2} at pH 9.

As a control experiment, we tested the stability of the bilayers in the presence of 0.5 mM Me-β-CD at each pH value, and found that Me-β-CD does not adsorb on the membrane surface or cause any changes in membrane structure or composition over a period of several hours. This data is available in the Supporting Information. Contrary to the assumption that cyclodextrins activate PLA_2 by extracting the fatty acid (*12*), Me-β-CD predominantly facilitated solubilization of the lyso-lipid. Only 22% of the oleic acid/oleate formed was coextracted with the lyso-lipid at pH 9. This result is not surprising considering that the lyso-lipid with its large zwitterionic headgroup has a much higher critical micellization concentration (cmc = 7 μM) (*35*) than the fatty acid (~10 pM for un-ionized oleic acid if extrapolated from the cmc of decenoic acid, which is approximately 10 nM (*36*)). At pH 7−9, the oleic acid and oleate also dimerize into acid−soap complexes, which stabilize the bilayer geometry and increase the apparent pK_a, so particularly when there are no counterions present, the solubility of the complexes is orders of magnitude lower than the solubility of the lyso-lipid. In our experiments, the volume of the buffer solution was large enough to accommodate approximately 1400 times the amount of the lyso-lipid solubilized from the supported membrane before reaching the cmc. In addition, it may be that the cis-double bond of oleic acid is more difficult to accommodate in the hydrophobic cavity of Me-β-CD (which has a diameter of ~0.8 nm) than the straight saturated palmitoyl chain of the lyso-lipid.

DISCUSSION

The thicknesses of the fatty acid layers (21−23 Å) after PLA_2 hydrolysis are much smaller than the length of two oleic acid molecules (C18:1cis9 ~ 15 Å), suggesting that severe tilting of the bilayer (44−50°) or interdigitation of the chains occurs or that the molecules flip to form a monolayer with the headgroups facing the silicon support. The formation of a monolayer would certainly be consistent with the presence of PLA_2 at the layer surface after hydrolysis because PLA_2 has a strong and irreversible interaction with hydrophobic monolayers (*26*). Fatty acid flip-flop would also be consistent with the lipid flip-flop rate observed in fluid supported bilayers (*37*), which occurs on a 10−20 min time scale. Interdigitation is unlikely for the unsaturated oleic acid chains, but tilting could be caused as a result of the decrease in lipid coverage on the support surface. It is not possible to determine the precise structure of the fatty acid layers from the current measurements, but we hope to pursue this question in the future by using partially deuterated fatty acids.

The initial lipid and final fatty acid amounts and lipid-PLA_2 ratios are plotted in Figure 3 with and without Me-β-CD. In both cases, the lipid to PLA_2 ratio decreases with increasing pH, indicating a stronger affinity of the enzyme for the membrane, as

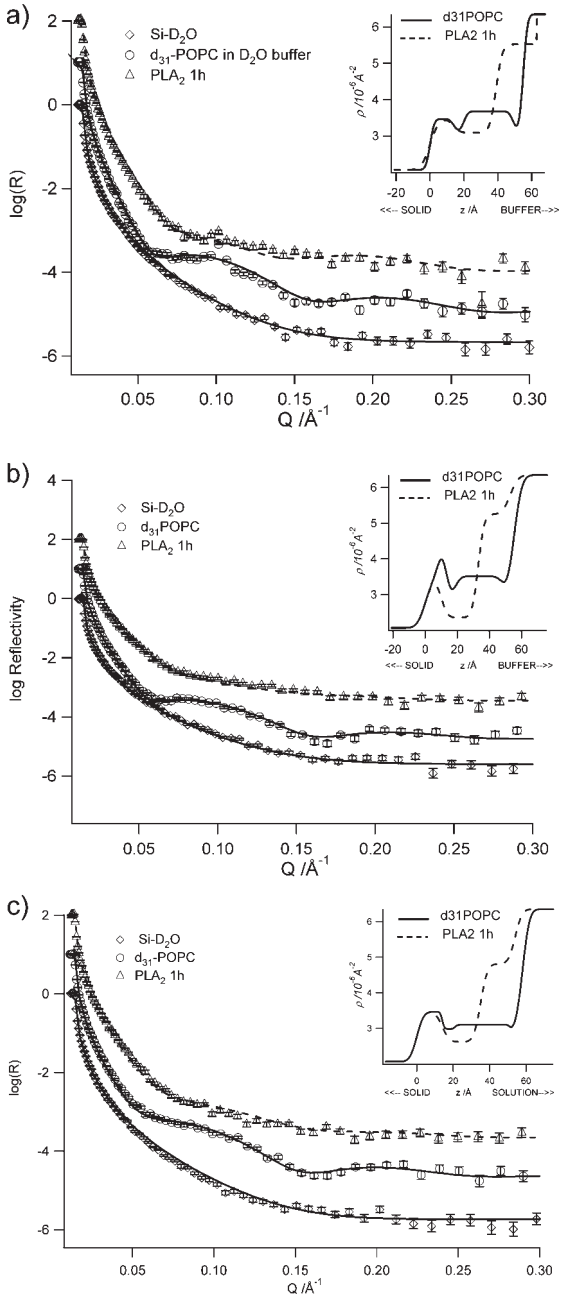

FIGURE 2: Neutron reflectivity recorded during POPC-d_{31} hydrolysis in the presence of 0.5 mg/mL Me-β-CD: (a) at pH 5, (b) pH 7.4, and (c) pH 9 after 1 h of PLA_2 exposure, after which no more changes were observed in the reflectivity profiles. The fitted reflectivity curves (lines) and scattering length density profiles (in insets) correspond to the parameters in Table 3.

expected when the degree of fatty acid ionization increases. In the absence of Me-β-CD, slightly more PLA_2 is recruited to the membrane as the reaction progresses at pH 9 than at pH 7.4, whereas with the Me-β-CD, the reaction rate is so fast at all pH that only the final fatty acid-PLA_2 ratio could be measured, which also decreased with pH.

A closer look at the data reveals more subtle differences in the behavior in the presence and absence of Me-β-CD. With Me-β-CD, the amount of PLA_2 at the membrane surface at pH 5 is much higher than that in the absence of Me-β-CD, which seems counterintuitive since the lyso-lipid extraction should not alter the enzyme−membrane interaction when the fatty acid is uncharged (the apparent pK_a of long chain fatty acids is 8−9 in an aggregated membrane) (*32*). At pH 7.4, it may be that a small number of the fatty acids produced are ionized, but at pH 9 they are fully ionized, which is consistent with the increase in the reaction rate from pH 7.4 to 9 being accompanied by more PLA_2 at the membrane interface. The enzyme amount also increases during the reaction faster at pH 9 than at pH 7.4.

Another possible cause for the pH-dependent activity are changes in ionization state of the enzyme. The *Naja mossambica mossambica* PLA_2 sequence has several ionizable groups (*38*), of which three histidines (p$K_a \sim 6.2$) change their ionization state going from pH 9 to pH 5. It is also possible that in these experiments some of the seven aspartates (pK_a 4.5) and six glutamic acids (pK_a 4.6) of PLA_2 were partially uncharged, as pH 5 in D_2O corresponds to pD 4.6(*39*). The net enzyme charge (including the Ca^{2+} cofactor) estimated from the pK_a's of all residues is neutral at pH 9 (when the N-terminus is deprotonated), +1 at pH 7.4, but becomes increasingly positive at pH 5 (+10, assuming that the Asp and Glu residues have a 50% degree of ionization). The positively charged residues (Lys, Arg) that are largely responsible for the activation of PLA_2 by negatively charged lipids or fatty acids are clustered on the interfacial binding face (*40*), but they do not change their ionization state within the pH 5−9 range. However, as the substrate membrane is zwitterionic, a net positive charge on the enzyme should not lead to repulsion between the substrate and enzyme.

The low pH inactivity could be explained by inhibition of the active site mechanism of PLA_2, which relies on nucleophilic attack on the lipid sn-2 ester bond by a water molecule, catalyzed by proton removal from the water by His48(*41*, *42*). At pH 5, the His48 is protonated, and therefore it should not be able to act as the catalytic base. However, activation by Me-β-CD, which cannot interact with the enzyme active site directly due to its size, shows that the hydrolytic mechanism of PLA_2 is not disabled at pH5. In general, PLA_2 is inhibited by phosphonate transition state analogues at low pH, which has been found to be based on hydrogen bonding of the catalytic histidine with the phosphate group (*43*). It has also been shown that the protonation of His48 promotes the binding of PLA_2 to phosphorylcholine surfactant micelles (*44*, *45*). This suggest that PLA_2 binding to the lipid phosphate should become stronger when His48 is protonated, but it is not reflected in the amount of the enzyme bound to the membrane, which is lowest at pH 5. Cleavage of the sn-2 bond is also not inhibited, because extraction of the lyso-lipid by Me-β-CD leads to full activation. The results of the present work therefore suggest that the mechanism by which PLA_2 can cleave the sn-2 acyl bond at low pH is not yet fully understood.

The results also raise a question about the mechanism by which Me-β-CD activates PLA_2. Me-β-CD does not interact with or penetrate the membrane, and extraction of the lyso-lipid directly from the membrane is therefore unlikely if PLA_2 is unable to release it. The substrate lipids are not encapsulated by Me-β-CD. PLA_2 binding to the membrane is weak at pH5, suggesting that it operates via the hopping mechanism (*46*), illustrated in Figure 4. At low pH, in the weak substrate-binding limit, membrane-bound PLA_2 is in rapid equilibrium with the solution phase, and "hops" from site to site on the membrane surface between catalytic cycles. The enzyme−product complex unbinds from the membrane after hydrolyzing a substrate lipid, after which Me-β-CD extracts the lyso-lipid from PLA_2, which allows the enzyme to return to the catalytic cycle. In the absence of Me-β-CD, the PLA_2 is unable to release the lyso-lipid products

Table 3: Structural Parameters of POPC-d_{31} Bilayers before and after PLA_2 Hydrolysis at pH 5, pH 7, and pH 9 in the Presence of 0.5 mM Me-β-CD[a]

description	layer	ρ/ 10^{-6} Å^{-2}[b]	ρ_a/ 10^{-6} Å^{-2}[c]	t/ Å[d]	ϕ[e]	A_a/ Å[f]	Γ/ μmol m^{-2}[g]
POPC-d_{31} pH 5	head	1.8	3.1 ± 0.2	6 ± 1	0.71 ± 0.05	76 ± 21	4.4 ± 0.4
	chains	3.2 ± 0.15	3.7 ± 0.1	29 ± 2	0.84 ± 0.02	77 ± 8	
POPC-d_{31} pH 5 + PLA_2 + Me-β-CD 1 h	FA	−0.3	3.1 ± 0.1	25 ± 2	0.49 ± 0.02	38 ± 5	4.4 ± 0.4
	PLA_2	3.6	5.5 ± 0.2	24 ± 3	0.30 ± 0.07	2100 ± 800	0.08 ± 0.3
POPC-d_{31} pH 7	head	1.8	2.7 ± 0.2	6 ± 1	0.80 ± 0.05	67 ± 18	5.0 ± 0.5
	chains	3.2 ± 0.15	3.5 ± 0.	31 ± 2	0.90 ± 0.02	67 ± 6	
POPC-d_{31} pH 7 + PLA_2 + Me-β-CD 1 h	FA	−0.3	2.9 ± 0.1	23 ± 2	0.60 ± 0.02	34 ± 4	4.9 ± 0.5
	PLA_2	3.6	4.9 ± 0.2	20 ± 3	0.40 ± 0.07	1900 ± 700	0.1 ± 0.03
POPC-d_{31} pH 9	head	1.8	3.5 ± 0.2	7 ± 1	0.76 ± 0.05	61 ± 14	5.4 ± 0.5
	chains	2.8 ± 0.15	2.8 ± 0.1	30 ± 2	1.00 ± 0.02	62 ± 6	
POPC-d_{31} pH 9 + PLA_2 + Me-β-CD 1 h	FA[g]	−0.3	2.6 ± 0.1	21 ± 2	0.56 ± 0.02	40 ± 6	4.2 ± 0.4
	PLA_2	3.6	5.4 ± 0.2	19 ± 3	0.56 ± 0.07	1450 ± 500	0.1 ± 0.03

[a] Where only one headgroup layer is given, the outer and inner layers were found to be identical. [b] ρ = molecular scattering length density. Where no error limits for ρ are given, the parameters were fixed in our data-analysis. [c] ρ_a = total scattering length density of layer a, including D_2O. Head 1 refers to the inner headgroup layer facing the silicon surface. [d] t = layer thickness. [e] ϕ = lipid volume fraction. [f] A_a is the area available per molecule. [g] Γ is the lipid surface coverage. [h] FA = fatty acid. This layer is assumed to be composed only of oleic acid, and the values of A_a and Γ have been calculated using the molecular volume of 467 Å^3 corresponding to it.

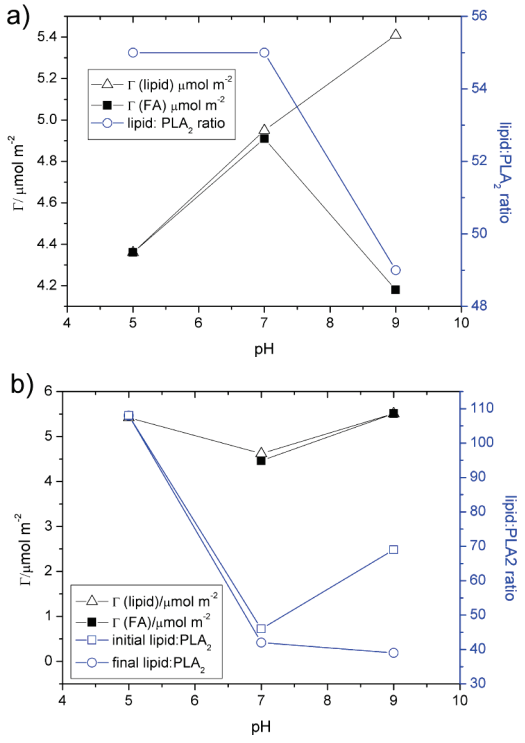

FIGURE 3: Initial lipid surface concentration, final fatty acid concentration and initial/final lipid: PLA_2 ratios as a function of pH (a) in the absence and (b) presence of 0.5 mM Me-β-CD (*values at pH 7.4 have been published previously(*25*) and are presented here for comparison).

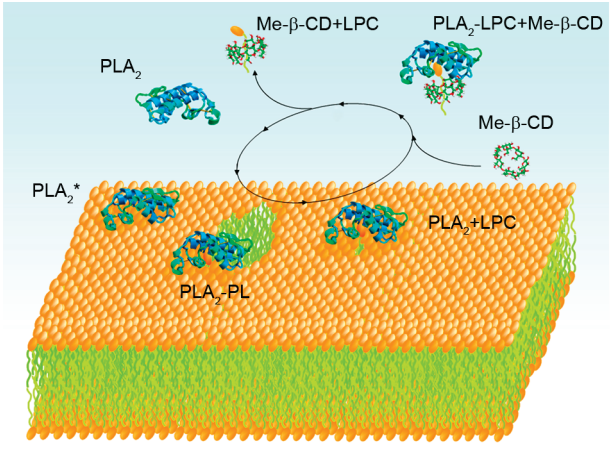

FIGURE 4: PLA_2 activation by Me-β-CD during the hopping mechanism: As weakly bound PLA_2 unbinds from the substrate membrane after hydrolyzing a lipid substrate, the lyso-lipid is extracted from PLA_2 by Me-β-CD, which releases the enzyme back to the catalytic cycle.

and remains inactive. An alternative mechanism would be that the lyso-lipid, once formed, partitions out of the membrane and inhibits PLA_2 in solution, but this would not explain the pH 5 results − no lyso-lipid is observed to leave the membrane in the absence of Me-β-CD.

The fatty acid product either remains in the membrane when the PLA_2−lysolipid complex unbinds, or partitions into it as soon as it is released from the active site − it has been shown from crystal structures of PLA_2−product complexes that binding of lyso-lipid and fatty acid to the same enzyme molecule may be mutually exclusive(*47*).

At pH 7.4 and 9, the inhibiting effect of lyso-lipid is decreased as His48 is unprotonated, and the enzyme becomes more strongly bound to the membrane with increasing ionization of the fatty acid. Me-β-CD still has an activating effect, but it is possible that it extracts the lyso-lipid directly out of the membrane, in addition to or instead of encapsulating it in solution. However, because the hydrolysis rate is increased by the Me-β-CD-facilitated removal of the lyso-lipid, this suggests that its release from the enzyme or membrane still has a rate-limiting effect.

The remainder of the mechanism is consistent with previous observations. Lyso-lipid extraction by Me-β-CD also facilitates the enzyme−membrane interaction by decreasing the lipid density, thus giving the enzyme easier access to the acyl bonds and the hydrophobic chains(*25*). The removal of the lyso-lipids allows aggregation of the fatty acids which, in turn, increases the local membrane heterogeneity (*20*) and promotes PLA_2 adsorption. At pH 9 in the presence of Me-β-CD, there is a small difference (22 mol %) in the final fatty acid concentration and the original lipid concentration, which shows that only a small fraction of the ionized fatty acids are coextracted with the lyso-lipid at alkaline pH. The fatty acid solubilization is not rate-limiting as PLA_2 is also active at pH 9 in the absence of Me-β-CD.

CONCLUSION

The pH dependence of phospholipase A_2 activity in the presence and absence of Me-β-CD was investigated by neutron reflection. The low pH inhibition of PLA_2 is consistent with protonation of the catalytic histidine and inhibition by lyso-lipid, but activation by Me-β-CD shows that the catalytic site of the enzyme is not fully disabled. At low pH, Me-β-CD activation occurs by extraction of the lyso-lipid during the hopping mechanism of PLA_2, outside the membrane surface. This is to our knowledge the first time that the product-dependent activation and inhibition of PLA_2 has been by investigated in situ by direct structure−activity measurements, and the results demonstrate the importance of measuring membrane structure and composition concurrently with enzyme activity in interfacial enzyme catalysis.

ACKNOWLEDGMENT

H.W. thanks Drs. John Webster and Robert Cubitt for their assistance with the neutron reflection experiments at the ISIS Neutron Facility, and Institute Laue Langevin, respectively.

SUPPORTING INFORMATION AVAILABLE

Reflectivity simulations of the removal of both products (Figure 1S) and only the fatty acid (Figure 2S); measurement of Me-β-CD interaction with POPC-d_{31} in the absence of PLA_2 (Figures 3S−5S). This material is available free of charge via the Internet at http://pubs.acs.org

REFERENCES

1. Six, D. A., and Dennis, E. A. (2000) The expanding superfamily of phospholipase A(2) enzymes: classification and characterization. *Biochim. Biophys. Acta, Mol. Cell Biol. Lipids 1488*, 1–19.
2. Balsinde, J., Winstead, M. V., and Dennis, E. A. (2002) Phospholipase A2 regulation of arachidonic acid mobilization. *FEBS Lett. 531*, 2–6.
3. Leslie, C. C. (2004) Regulation of the specific release of arachidonic acid by cytosolic phospholipase A(2). *Prostaglandins Leukotrienes Essent. Fatty Acids 70*, 373–376.
4. Berg, O. G., Gelb, M. H., Tsai, M. D., and Jain, M. K. (2001) Interfacial enzymology: The secreted phospholipase A(2)-paradigm. *Chem. Rev. 101*, 2613–2653.
5. Jensen, U. B., and Simonsen, A. C. (2005) Shape relaxations in a fluid supported membrane during hydrolysis by phospholipase A2. *Biochim. Biophys. Acta, Biomembranes 1715*, 1–5.
6. Balashev, K., Jensen, T. R., Kjaer, K., and Bjornholm, T. (2001) Novel methods for studying lipids and lipases and their mutual interaction at interfaces. Part I. Atomic Force Microscopy. *Biochimie 83*, 387–397.
7. Sanchez, S. A., Bagatolli, L. A., Gratton, E., and Hazlett, T. L. (2002) A two-photon view of an enzyme at work: Crotalus atrox venom PLA (2) interaction with single-lipid and mixed-lipid giant unilamellar vesicles. *Biophys. J. 82*, 2232–2243.
8. Callisen, T. H., and Talmon, Y. (1998) Direct imaging by cryo-TEM shows membrane break-up by phospholipase A(2) enzymatic activity. *Biochemistry 37*, 10987–10993.
9. Burack, W. R., Dibble, A. R. G., Allietta, M. M., and Biltonen, R. L. (1997) Changes in vesicle morphology induced by lateral phase separation modulate phospholipase A(2) activity. *Biochemistry 36*, 10551–10557.
10. Cajal, Y., Alsina, M. A., Berg, O. G., and Jain, M. K. (2000) Product accumulation during the lag phase as the basis for the activation of phospholipase A(2) on monolayers. *Langmuir 16*, 252–257.
11. Cajal, Y., Berg, O. G., and Jain, M. K. (2004) Origins of delays in monolayer kinetics: Phospholipase A(2) paradigm. *Biochemistry 43*, 9256–9264.
12. Ivanova, M., Verger, R., and Panaiotov, I. (1997) Mechanisms underlying the desorption of long-chain lipolytic products by cyclodextrins: application to lipase kinetics in monolayer. *Colloids Surf., B: Biointerfaces 10*, 1–12.
13. Jain, M. K., and Jahagirdar, D. V. (1985) Action of phospholipase-A2 on bilayers - Effect of fatty-acid and lysophospholipid additives on the kinetic-parameters. *Biochim. Biophys. Acta 814*, 313–318.
14. Jain, M. K., and Dehaas, G. H. (1983) Activation of phospholipase-A2 by freshly added lysophospholipids. *Biochim. Biophys. Acta 736*, 157–162.
15. Apitzcastro, R., Jain, M. K., and Dehaas, G. H. (1982) Origin of the latency phase during the action of phospholipase-A2 on unmodified phosphatidylcholine vesicles. *Biochim. Biophys. Acta 688*, 349–356.
16. Jain, M. K., and Maliwal, B. P. (1985) The Environment of tryptophan in pig pancreatic phospholipase-A2 bound to bilayers. *Biochim. Biophys. Acta 814*, 135–140.
17. Burack, W. R., Yuan, Q., and Biltonen, R. L. (1993) Role of lateral phase-separation in the modulation of phospholipase-A2 activity. *Biochemistry 32*, 583–589.
18. Lichtenberg, D., Romero, G., Menashe, M., and Biltonen, R. L. (1986) Hydrolysis of dipalmitoylphosphatidylcholine large unilamellar vesicles by porcine pancreatic phospholipase A2. *J. Biol. Chem. 261*, 5334–5340.
19. Bell, J. D., and Biltonen, R. L. (1989) The temporal sequence of events in the activation of phospholipase-A2 by lipid vesicles - studies with the monomeric enzyme from *Agkistrodon-Piscivorus-Piscivorus*. *J. Biol. Chem. 264*, 12194–12200.
20. Honger, T., Jorgensen, K., Biltonen, R. L., and Mouritsen, O. G. (1996) Systematic relationship between phospholipase A(2) activity and dynamic lipid bilayer microheterogeneity. *Biochemistry 35*, 9003–9006.
21. Hoyrup, P., Jorgensen, K., and Mouritsen, O. G. (2002) Nano-scale structure in membranes in relation to enzyme action - computer simulation vs. experiment. *Comput. Phys. Commun. 147*, 313–320.
22. Bell, J. D., Burnside, M., Owen, J. A., Royall, M. L., and Baker, M. L. (1996) Relationships between bilayer structure and phospholipase A (2) activity: Interactions among temperature, diacylglycerol, lysolecithin, palmitic acid, and dipalmitoylphosphatidylcholine. *Biochemistry 35*, 4945–4955.
23. Bent, E. D., and Bell, J. D. (1995) Quantification of the interactions among fatty acid, lysophosphatidylcholine, calcium, dimyristoylphosphatidylcholine vesicles, and phospholipase A2. *Biochim. Biophys. Acta, Lipids Lipid Metab. 1254*, 349–360.
24. Henshaw, J. B., Olsen, C. A., Farnbach, A. R., Nielson, K. H., and Bell, J. D. (1998) Definition of the specific roles of lysolecithin and palmitic acid in altering the susceptibility of dipalmitoylphosphatidylcholine bilayers to phospholipase A2. *Biochemistry 37*, 10709–10721.
25. Wacklin, H. P., Tiberg, F., Fragneto, G., and Thomas, R. K. (2007) Distribution of reaction products in phospholipase A2 hydrolysis. *Biochim. Biophys. Acta, Biomembranes 1768*, 1036–1049.
26. Vacklin, H., Tiberg, F., Fragneto, G., and Thomas, R. K. (2005) Phospholipase A2 hydrolysis of supported phospholipid bilayers: a neutron reflectivity and ellipsometry study. *Biochemistry 44*, 2811–2821.
27. Vacklin, H. P., Tiberg, F., Fragneto, G., and Thomas, R. K. (2005) Composition of supported model membranes determined by neutron reflection. *Langmuir 21*, 2827–2837.
28. Nelson, A. (2006) Co-refinement of multiple-contrast neutron/X-ray reflectivity data using MOTOFIT. *J. Appl. Crystallogr. 39*, 273–276.
29. Heavens, O. S. (1955) Optical properties of Thin Films , Butterworths, London.
30. Slotte, J. P., and Illman, S. (1996) Desorption of fatty acids from monolayers at the air/water interface to cyclodextrin in the subphase. *Langmuir 12*, 5664–5668.
31. Ivanova, M. G., Ivanova, T., Verger, R., and Panaiotov, I. (1996) Hydrolysis of monomolecular films of long chain phosphatidylcholine by phospholipase A(2) in the presence of beta-cyclodextrin. *Colloids Surf., B-Biointerfaces 6*, 9–17.
32. Kanicky, J. R., and Shah, O. D. (2003) Effect of premicellar aggregation on the pKa of fatty acid soap solutions. *Langmuir 19*, 2034–2038.
33. Naik, P. V., and Dixit, S. G. (2008) Ufasomes as plausible carriers for horizontal gene transfer. *J. Dispersion Sci. Technol. 29*, 804–808.
34. Alahverdjieva, V., Ivanova, M., Verger, R., and Panaiotov, I. (2005) A kinetic study of the formation of [beta]-cyclodextrin complexes with monomolecular films of fatty acids and glycerides spread at the air/water interface. *Colloids Surf., B: Biointerfaces 42*, 9–20.
35. Stafford, R. E., Fanni, T., and Dennis, E. A. (1989) Interfacial properties and critical micelle concentration of lysophospholipids. *Biochemistry 28*, 5113–5120.
36. Neys, B., and Joos, P. (1998) Equilibrium surface tensions and surface potentials of some fatty acids. *Colloids Surf., A: Physicochem. Eng. Aspects 143*, 467–475.
37. Liu, J. a. C. (2005) 1,2-Diacyl-phosphatidylcholine flip-flop measured directly by sum-frequency vibrational spectroscopy. *Biophys. J. 89*, 2522–2532.

38. Arni, R. K., and Ward, R. J. (1996) Phospholipase A(2) - A structural review. *Toxicon 34*, 827–841.
39. Kaiser, B. L., and Kaiser, E. T. (1969) Effect of D_2O on the carboxypeptidase-catalyzed hydrolysis of *O*-(*trans*-cinnamoyl)-L-beta-phenyllacta Te and N-(N-benzo ylglycyl)-L-phenylalanine. *Proc. Natl. Acad. Sci. U.S.A. 64*, 36–41.
40. Scott, D. L., Mandel, A. M., Sigler, P. B., and Honig, B. (1994) The electrostatic basis for the interfacial binding of secretory phospholipases A2. *Biophys. J. 67*, 493–504.
41. Scott, D. L., White, S. P., Otwinowski, Z., Yuan, W., Gelb, M. H., and Sigler, P. B. (1990) Interfacial catalysis - the mechanism of phospholipase-A2. *Science 250*, 1541–1546.
42. Dijkstra, B. W., Drenth, J., and Kalk, K. H. (1981) Active-site and catalytic mechanism of phospholipase-A2. *Nature 289*, 604–606.
43. Yu, L., and Dennis, E. A. (1991) Critical role of a hydrogen bond in the interaction of phospholipase A2 with transition-state and substrate analogues. *Proc. Natl. Acad. Sci. U.S.A. 88*, 9325–9329.
44. Ikeda, K., Sano, S.-i., Teshima, K., and Samejima, Y. (1984) pH dependence of the binding constant of a phospholipase A2 from *Agkistrodon halys blomhoffii* venom to micelles of *n*-hexadecylphosphorylcholine. *J. Biochem. 96*, 1427–1436.
45. Donne-Op, G. M., Hille, J. D. R., Dijkman, R., De Haas, G. H., and Egmond, M. R. (1981) Binding of porcine pancreatic phospholipase A2 to various micellar substrate analogs. The involvement of histidine-48 and aspartic acid-49 in the binding process. *Biochemistry 20*, 4074–4078.
46. Jain, M. K., and Berg, O. G. (1989) The kinetics of interfacial catalysis by phospholipase-A2 and regulation of interfacial activation - hopping versus scooting. *Biochim. Biophys. 1002*, 127–156.
47. Pan, Y. H., Yu, B. Z., Berg, O. G., Jain, M. K., and Bahnson, B. J. (2002) Crystal structure of phospholipase A(2) complex with the hydrolysis products of platelet activating factor: Equilibrium binding of fatty acid and lysophospholipid-ether at the active site may be mutually exclusive. *Biochemistry 41*, 14790–14800.